The fcc–bcc Bain path in In–Sn and related alloys at ambient and high pressure

2009 J. Phys.: Condens. Matter 21 095702

(http://iopscience.iop.org/0953-8984/21/9/095702)

J. Phys.: Condens. Matter **21** (2009) 095702 (5pp) doi:10.1088/0953-8984/21/9/095702

The fcc–bcc Bain path in In–Sn and related alloys at ambient and high pressure

Valentina F Degtyareva

Institute of Solid State Physics, Russian Academy of Sciences, Chernogolovka, 142432, Russia

Received 2 December 2008, in final form 14 January 2009
Published 4 February 2009
Online at stacks.iop.org/JPhysCM/21/095702

Abstract

Experimental high-pressure structural studies on an In–Sn alloy containing 8 at.% Sn reveal an isostructural transition of a face-centered tetragonal phase at pressures above 15 GPa with a switch of the axial ratio from $c/a > 1$ to $c/a < 1$. Such tetragonal phases in binary alloys based on In and Sn are analyzed in relation to the Bain path, i.e. a transformation between a face-centered cubic (fcc) and a body-centered cubic (bcc) structure. Variation of the axial ratio c/a in these phases correlates with the average number of valence electrons per atom in an alloy. A common Bain path from fcc to bcc is discussed within a nearly-free-electron model of Brillouin-zone–Fermi-sphere interactions.

1. Introduction

Indium crystallizes in a tetragonal structure which is unique among the metallic elements, usually adopting high-symmetry closely packed structures such as face-centered cubic (fcc), body-centered cubic (bcc) and hexagonal close-packed (hcp) structures [1]. The tetragonal structure of In is a slight distortion of fcc with an axial ratio $c/a = 1.076$ of a tetragonal face-centered cell (fct). The standard crystallographic description of this structure is body-centered tetragonal (bct), space group $I4/mmm$, with two atoms in the unit cell placed at (0, 0, 0) and (1/2, 1/2, 1/2), Pearson symbol $tI2$ ($c/a = 1.521$ in the bct setting). The structural transformation from fcc to bcc is known as the Bain path [2]. Both structures, fcc and bcc, can be represented by a common tetragonal body-centered cell (bct) with the axial ratio $c/a = \sqrt{2}$ for fcc and $c/a = 1$ for bcc (see figure 1, inset).

The axial ratio of the In-type structure is changed by alloying of In with neighboring elements, as shown in figure 1 which summarizes the data on ambient pressure phases [3, 4]. These phases are site-disordered, and it is convenient to consider the degree of tetragonal distortion as a function of the number of valence electrons per atom (z). Alloying of In with a divalent metal, Cd or Hg, results in a decrease of c/a to 1.05 at $z = 2.95$. An addition of ~6 at.% Cd or Hg ($z = 2.94$) stabilizes the fcc phase. On the other hand, alloying of In with a tetravalent metal, Sn or Pb, results first in an increase of c/a to 1.09 and then in a jump of c/a from >1 to <1, with c/a equal to 0.933 or 0.917 with the addition of 14 at.% Pb or Sn, respectively (this corresponds to the critical composition $z \sim 3.12$ electron/atom). The values of c/a in relation to the electron concentration follow Svechkarev's plot (solid lines) [5] as discussed below.

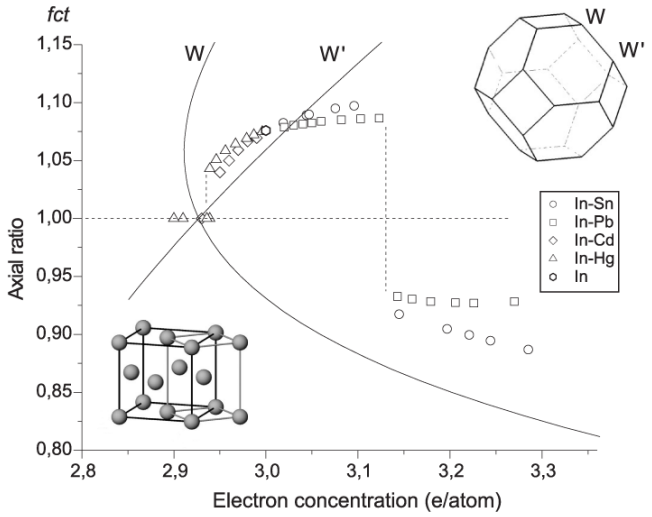

Figure 1. Variation of the axial ratio c/a as a function of the electron concentration, z, for the tetragonal phases, fct, in In-based alloys. Data are shown for ambient pressure phases [4]. Solid curves represent the degree of tetragonal distortion of fcc (c/a) calculated for the condition when the Brillouin zone corners of type W and W′ (shown in the upper inset) are in contact with the free-electron Fermi sphere as a function of z [5]. Structural relationship between fcc (dark lines) and bcc (gray lines) is shown in the lower inset.

High-pressure studies on indium [6–9] have shown the stability of the tetragonal phase up to $P \sim 45$ GPa with a flat

maximum of c/a at ~24 GPa. At pressures up to ~93 GPa, the structure of In remained close to the initial tetragonal structure, with a possible slight orthorhombic distortion [9]. For the lighter group-III element Ga, the same tetragonal In-type structure was found [10–12] to be stable under pressures above 14 GPa with $c/a = 1.1$, which decreased continuously under pressure, and above 120 GPa Ga transformed to fcc [11].

The crystal structure of In with the tetragonal distortion of fcc was the subject of theoretical considerations [13–16]. The tetragonal distortion of the cubic structure is shown to be accompanied by an increase of hybridization of the 5s and 5p valence electron bands. Structural sequences in In-based alloys with Cd and Sn are explained by 'an enhancement of s–p hybridization with increasing VEC' (valence electron concentration) [17]. Recently, the temperature–pressure–concentration evolution of the crystal lattice of In-based alloys has been analyzed in the framework of phenomenological theory on a symmetry basis considering the c/a ratio as an order parameter [18].

Another approach to the explanation of the structural distortion in In and In-based alloys is focused on the interaction between the Brillouin zone (BZ) boundaries and the Fermi surface (FS). As was discussed by Heine and Weaire [19], experimental correlation between c/a and the electron-per-atom ratio z in In alloys indicates the electronic reason for the structural distortion of In and 'details of Fermi-surface–Brillouin-zone interactions play a significant role'. It was suggested by Svechkarev [5] 'that it is favorable for corners of the Brillouin zone to touch the Fermi sphere'. Figure 1 represents Svechkarev's plot within a nearly-free-electron model for c/a in correlation with z corresponding to FS touching BZ corners of either W or W′ type. Effects of the FS–BZ interactions for simple (sp) metals are considered recently in [20]. These effects should increase under pressure because the electronic band structure contribution to the crystal energy becomes more important on compression compared to the electrostatic term. Thus, the ambient pressure correlation of c/a and z is expected to be modified under high pressure with respect to the increase in the FS–BZ interaction.

In this paper, experimental results of high-pressure studies on an In–Sn alloy with 8 at.% Sn are presented with the observation of an isostructural transition of the fct phase with a switch in the axial ratio from $c/a > 1$ to $c/a < 1$, which was predicted to occur under pressure. We analyze these results together with the sequence of tetragonal phases in In–Sn and related alloys observed in previous high-pressure studies [21–26]. A common Bain path from fcc to bcc is discussed within a nearly-free-electron model of Brillouin-zone–Fermi-sphere interactions.

2. Experimental high-pressure studies on the $In_{0.92}Sn_{0.08}$ alloy

In-based alloys near the critical composition $z \sim 3.12$ electron/atom (see figure 1) are interesting for high-pressure studies because the pressure should increase the FS–BZ interaction and shift ambient pressure relations between c/a and z. In the previous paper on In–Pb alloys [26], samples with compositions

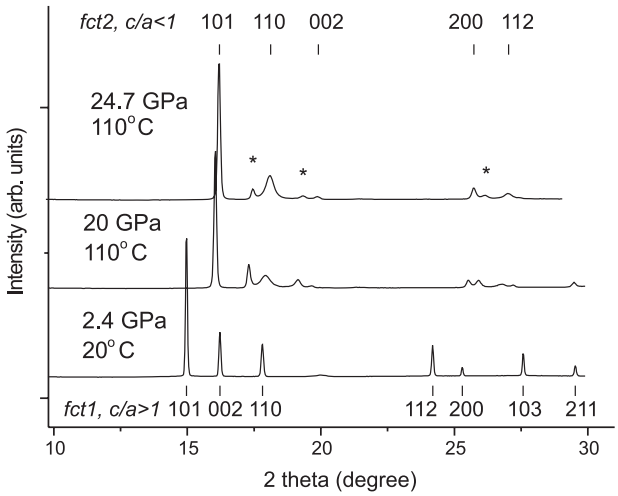

Figure 2. Selected diffraction patterns of the $In_{0.92}Sn_{0.08}$ alloy at different pressures ($\lambda = 0.7112$ Å). The low-pressure phase is fct1, $c/a > 1$ (pattern at 2.4 GPa), the high-pressure phase is fct2, $c/a < 1$ (pattern at 24.7 GPa). In the intermediate pressure range two phases, fct1 and fct2, coexist (pattern at 20 GPa). Calculated peak positions and indices are indicated for both phases; asterisks in the upper pattern indicate the peaks from the remaining low-pressure phase. Lattice parameters are summarized in table 1.

10, 15 and 22 at.% Pb were selected for high-pressure studies, covering the critical region of z where the c/a changes from >1 to <1 for the fct phase at ambient pressure. A transformation of the tetragonal phase under pressure was expected: however, it was not clear at that time in what direction c/a should be changed under pressure. The observed transition in the $In_{90}Pb_{10}$ alloy with the change of c/a from >1 to <1 is in agreement with the increase of the FS–BZ interaction, as the value of c/a obtained under pressure approaches Svechkarev's plot. Based on these results a similar transformation was predicted for the In–Sn alloys. For high-pressure studies, the $In_{0.92}Sn_{0.08}$ alloy was selected with the ambient pressure fct phase with $c/a = 1.093$ corresponding to $z = 3.08$. An alloy preparation method was the same as described previously [26].

In situ x-ray diffraction high-pressure studies were performed at the Swiss–Norwegian beamline (BM1A) of the European Synchrotron Radiation Facility (ESRF). A monochromatic beam at wavelength $\lambda = 0.7112$ Å was used with data collection on an image plate detector (MAR345). Details of the experimental methods are described in [18]. Diffraction measurements were performed up to a maximum pressure of 35 GPa at room temperature and with heating at 110 °C. The heating was used to accelerate the phase transformation and to release stresses in the alloy under quasi-hydrostatic pressure; and the temperature 110 °C was selected to be slightly below the melting temperature ~150 °C of the $In_{0.92}Sn_{0.08}$ alloy at ambient pressure.

Selected diffraction patterns of the $In_{0.92}Sn_{0.08}$ alloy at different pressures are shown in figure 2 demonstrating a gradual transition of the fct phase with $c/a > 1$ to another fct phase with $c/a < 1$ through a two-phase mixture. Data on lattice parameters for both fct phases are summarized in table 1. The axial ratio as a function of pressure is plotted in figure 3. The phase transition from fct, $c/a > 1$, to fct,

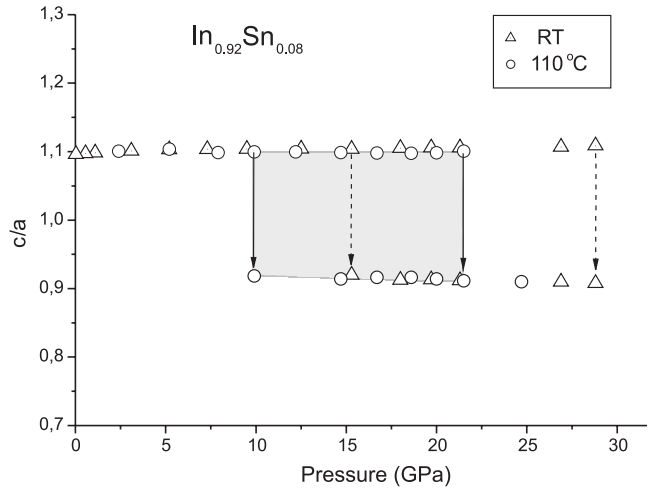

Figure 3. Variation of the axial ratio c/a for the tetragonal phases of the $In_{0.92}Sn_{0.08}$ alloy as a function of pressure at room temperature and at 110 °C. Two-phase regions (fct1 + fct2) are located between solid arrows at 110 °C (shaded area) and between dashed arrows at room temperature.

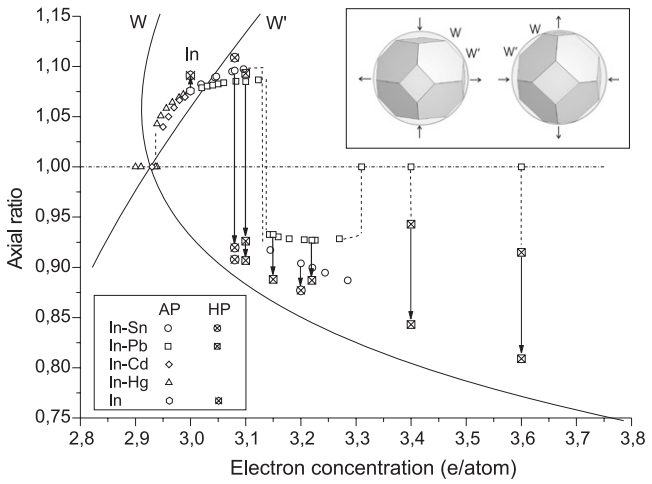

Figure 4. Variation of the axial ratio c/a for the tetragonal phases, fct, in In-based alloys as a function of the electron concentration, z. Small symbols are for ambient pressure (AP) [4] and large crossed symbols are for high pressure (HP) [23, 26]. Solid curves represent Svechkarev's plot. The Brillouin zones for the fct structures with $c/a > 1$ (left) and $c/a < 1$ (right) are shown in the inset, with the arrows indicating the direction of the deformation of the Brillouin zone from the fcc. The outwards arrows represent the shifts of the BZ planes due to the tetragonal deformation that provides the contact of W or W′ corners with the Fermi sphere.

Table 1. Structural characteristics of two tetragonal phases in the $In_{0.92}Sn_{0.08}$ alloy at ambient and high pressures. Both phases have a body-centered tetragonal structure, space group $I4/mmm$, Pearson symbol $tI2$. Axial ratio c/a is given for the bct and fct settings. (Note: the uncertainty of the data is within the last digit.)

	Lattice parameters for body-centered tetragonal cell (bct)				
Pressure (GPa)	a (Å)	c (Å)	c/a	c/a (fct)	V_{at} (Å^3)
0	3.2364	5.0048	1.5464	1.0933	26.207
2.4	3.2122	4.9998	1.556	1.1006	25.794
20.0	3.039	4.721	1.553	1.098	21.74
	3.2257	4.1697	1.293	0.914	21.69
24.7	3.1889	4.104	1.287	0.910	20.87

$c/a < 1$, begins at room temperature above 15 GPa and the two-phase region exists up to ∼30 GPa. With heating at 110 °C, the corresponding pressures are shifted down to ∼10 and ∼25 GPa, respectively. Thus, the two-phase region is dependent not only on kinetics but appears to be thermodynamically stable. In this region, the two phases have very minor differences in composition, approximately 2–3 at.%, as it is for the two-phase region on the ambient pressure diagram [3]. Atomic volumes for both fct phases in the two-phase region are very close to each other (see table 1).

3. The fcc–bcc Bain path in In–Sn and related alloys

The elements of the fifth row of the periodic table, Cd, In and Sn, are the nearest neighbors with a minimal difference in atomic size and electronegativity and differing mainly by the number of valence electrons. This allows us to consider the phase stability in the In–Sn and In–Cd alloys with only one main contribution from the electronic factor. These alloys cover a range of phases from fcc to bcc, including the intermediate tetragonal phases—the common Bain path—if one takes into account the ambient pressure as well as high-pressure phases. Phase sequences along the Bain path will be discussed in relation to fcc (In-rich alloys) and to bcc (Sn-rich alloys).

3.1. Tetragonal phases in the In-based alloys (fct close to fcc)

Experimentally observed tetragonal phases in In-based alloys at ambient and high pressure are presented in figure 4 showing c/a as a function of z. It is evident that, on the pressure increase (indicated by arrows), the values of c/a approach the calculated curves corresponding to the BZ corners of W or W′ type touching the Fermi sphere. The critical electron concentration, where the sign of the fcc deformation is changed from >1 to <1, is located near $z \sim 3.12$ at ambient pressure. This value is shifted with pressure to the lower z of 3.08–3.10, indicating that the contact of the FS with the W corners of the BZ is more energetically favorable on compression. This was found previously for the $In_{90}Pb_{10}$ alloy under pressure [26], and the same transition was predicted to occur under pressure in the $In_{0.92}Sn_{0.08}$ alloy and is found in the present study. The face-centered cubic phases in In–Pb alloys with 40 and 60 at.% Pb (corresponding to $z = 3.4$ and 3.6) were found to transform under pressure to an fct phase with the values of $c/a < 1$, approaching under pressure Svechkarev's plot [23].

3.2. Tetragonal phases in the Sn-rich alloys (bct close to bcc)

The common plot of the tetragonal phases along the fcc–bcc Bain path in In–Sn and related alloys is presented in figure 5. Extrapolation of Svechkarev's plot (W branch) to the higher z values gives the value $z \sim 4.2$ for $c/a = 0.707$ where

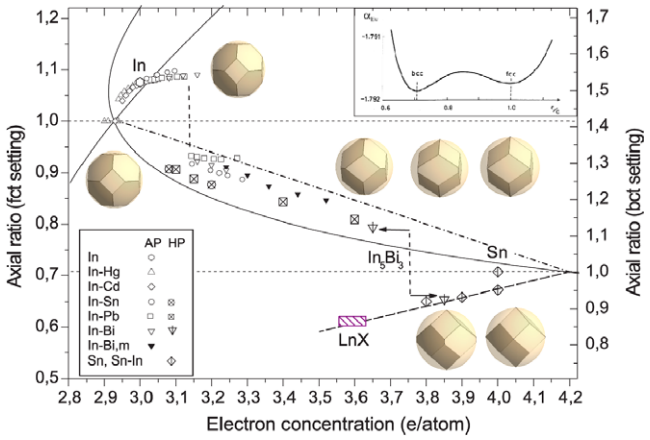

Figure 5. Common plot of tetragonal phases along the fcc–bcc Bain path in In–Sn and related alloys for ambient pressure (AP) and for high pressure (HP) [22–27]. Axial ratio c/a is given for fct (left) and bct (right) settings as a function of electron concentration z. FS–BZ configurations are shown for key cases (view along $[100]_{\rm fct}$ in upper and middle rows and along $[100]_{\rm bct}$ in the lower row). The straight dashed–dotted line corresponds to the expected direct (linear) fcc–bcc Bain path, vertical dashed lines indicate switches of c/a from >1 to <1 for fcc at $z \sim 3.12$ and for bcc at $z \sim 3.75$ (decomposition of In_5Bi_3). The straight dashed line represents the correlation of c/a with z (for the bct phase ($c/a < 1$)). Tetragonal phases for LnX are included in the plot assuming an 'effective' valence electron number $z \sim 3.5$ (see text). Inset shows the Ewald energy plot along c/a for tetragonal phases.

(This figure is in colour only in the electronic version)

bct = bcc. For the element Sn with $z = 4$, the known highest-pressure phase is bcc–stable at pressures above 40 GPa [27]. At lower pressures, however, before the transition to bcc, a bct structure exists in the pressure range ∼10–40 GPa with the axial ratio $c/a = 0.91$–0.94 [27]. The same bct phase was observed under pressure for InBi, for which z is also equal to 4 [28]. This bct structure is related to bcc compressed along the c axis. The data on bct phases with $c/a < 1$ for Sn and Sn-rich alloys ($z = 3.8$–3.9) [21, 22] are plotted in figure 5 and lie on the lower branch, discussed below.

Distortion of bcc to bct with $c/a < 1$ experimentally observed in Sn and Sn-based alloys in the region $3.8 < z < 4$ were discussed previously as originating also from FS–BZ interactions [21]. For the bcc structure with the atomic volume $V = a^3/2$, the Fermi sphere radius, $k_{\rm F} = (\frac{3\pi^2 z}{V})^{1/3}$, and lattice parameter in k-space, $\frac{2\pi}{a}$, for $z = 4$ are related by $\frac{k_{\rm F}}{2\pi/a} = (\frac{3}{\pi})^{1/3} < 1$. This means that $k_{\rm F} < \frac{2\pi}{a}$ or, in other words, the corners of the Brillouin zone formed by (110) planes of the bcc go outside the Fermi sphere. A Brillouin-zone–Fermi-sphere interaction can therefore favor a tetragonal distortion, to keep the corners of the BZ inside the FS. This model allows us to estimate c/a for the bct structure from the condition $\frac{2\pi}{a_t} \leqslant k_{\rm F}$, for which the corners of the BZ are inside the FS or just touching. This gives $\frac{c}{a} \leqslant \frac{3}{4\pi} z$ (see the straight dashed line in figure 5 representing the limiting case of $\frac{c}{a} = \frac{3}{4\pi} z$). Thus, $c/a \leqslant 0.96$ for $z = 4$ (Sn, InBi) and $c/a \leqslant 0.91$ for $z = 3.8$ (Sn–10 at.% Hg, Sn–20 at.% In), in good agreement with experimental values [21, 22].

3.3. The common fcc–bcc path

The transformation from fcc to bcc following the direct deformation (compression) along the c axis could be represented by a straight line (dashed–dotted line in figure 5) starting with fcc at $z = 3.94$ and ending with bcc at $z = 4.2$. This kind of linear fcc–bcc transformation can be expected if one takes into account only the electrostatic (or Ewald) energy contribution to the total structure energy. This is because the Ewald energy for the tetragonal structures plotted as a function of c/a has two minima, one for the fcc and another for the bcc structure, separated by a low and flat maximum [19] (see the inset in figure 5). The c/a values for metastable ambient pressure tetragonal phases of In–Bi alloys [4] indeed follow this linear plot of c/a versus z (z from 3.2–3.5). The high-pressure data on In–Pb and In–Sn alloys, however, give lower c/a values which lie closer to Svechkarev's plot (see figures 4 and 5).

Strong deviations from the linear fcc–bcc path occur near the critical regions of z at both ends of the path, where the c/a value changes the sign discontinuously. First, there is a discontinuity in c/a for the fct structure at $z \sim 3.12$. With the increase of pressure, this critical value is shifted to lower values ($z < 3.08$). The other critical value of z is nearly 3.75 where c/a switches from >1 to <1 for the bct phases (jumping around the value of $c/a = 1$ for the bcc structure). The middle and the left linear branches of the c/a variation as a function of z are separated by a large discontinuity in c/a at $z = 3.75$. High-pressure studies on the In_5B_3 compound [25] have shown the compound's decomposition into two bct phases of different composition with c/a equal to 1.126 and 0.923, located near those two branches as presented in figure 5.

Thus, it is observed experimentally that the c/a values at both ends of the Bain path do not follow the linear fcc–bcc plot, but rather show strong deviations and follow the lines calculated from the geometry of the BZ–FS interaction. This shows the importance of the BZ–FS interaction for the stabilization of the tetragonal distortions, with its role increasing on compression.

4. Conclusions

The isostructural transition of the tetragonal phase was experimentally observed under high pressure around 15 GPa in the In–Sn alloy with 8 at.% of Sn accompanied by a switch of c/a from 1.10 to 0.91 (in the fct setting). This means there is a change in the sign of the tetragonal distortion of fcc, corresponding to the change from elongation to compression along the [001] axis. Such a change in sign occurs in the In–Sn alloys at ambient pressure with the increase of the Sn content, i.e. increase in electron concentration, at the critical value of $z \sim 3.12$. This critical value is shifted under pressure to $z < 3.08$.

Variations of c/a as a function of z can be rationalized by considering the Fermi-sphere–Brillouin-zone configuration within the nearly-free-electron model. The change in the sign of the tetragonal deformation is associated with the change of FS contact to the BZ corners from W′ type to W type, which

becomes energetically more favorable with the increase of the valence electron contribution to the total structure energy.

A common Bain path from fcc to bcc as a variation of c/a along the electron concentration is constructed including data for the In–Sn and related alloys at ambient and high pressure. Experimentally observed bct phase sequences following Svechkarev's plot support the crucial role of the FS–BZ interaction which increases under compression and competes with the Ewald energy that prefers a linear transformation from fcc to bcc. The electronic contribution (band structure term) leads to strong deviations from the linear path with discontinuities in the axial ratio c/a as a function of z and switch of the sign of c/a from >1 to <1 at two critical values of electron concentration by approaching both cubic structures, fcc and bcc.

The behavior of c/a along the fcc–bcc path for sp metals considered on the basis of the valence electron energy might be useful for understanding the tetragonal structures in some compounds of lanthanides and actinides LnX and AnX, where X is a group V element, called pnictides. These compounds transform at high pressure from the NaCl-type structure to the CsCl-type structure via a tetragonal distorted CsCl-type [29]. This case can be considered as a diatomic equivalent of bcc and bct. Tetragonal phases of LnX can be placed on the common plot corresponding to bct with $c/a < 1$ at $z \sim 3.5$ on the lower branch in figure 5. Interestingly, such tetragonal distortion was not found at the similar transition from NaCl to CsCl for Ln and An compounds with group VI elements, chalcogenides. This fact supports that tetragonal distortions of CsCl-type structure in monopnictides are related to electronic reasons.

Acknowledgments

The author thanks Dr N I Novokhatskaja for the alloy preparation. Collaboration with V P Dmitriev, D Chernyshov and Y E Filinchuk is gratefully acknowledged. This work is supported by the Russian Foundation for Basic Research under grant no. 07-02-00901.

References

[1] Donohue J 1974 *The Structure of the Elements* (New York: Wiley)
[2] Bain E C 1924 *Trans. Am. Inst. Metall. Eng.* **70** 25
[3] Massalsky T B 1986 *Binary Alloy Phase Diagrams* (Metals Park, OH: American Society for Metals)
[4] Pearson W B 1964 *A Handbook of Lattice Spacings and Structures of Metals and Alloys* (Oxford: Pergamon)
Pearson W B 1967 *A Handbook of Lattice Spacings and Structures of Metals and Alloys* vol 2 (Oxford: Pergamon)
[5] Svechkarev I V 1964 *Zh. Eksp. Teor. Fiz.* **47** 961
Svechkarev I V 1965 *Sov. Phys.—JETP* **20** 643 (Engl. Transl.)
[6] Vereshchagin L F, Kabalkina C C and Troitskaja Z V 1964 *Dokl. Akad. Nauk SSSR* **158** 1061
Vereshchagin L F, Kabalkina C C and Troitskaja Z V 1965 *Sov. Phys.—Dokl.* **9** 894 (Engl. Transl.)
[7] Schulte O and Holzapfel W B 1993 *Phys. Rev.* B **48** 767
[8] Takemura K 1991 *Phys. Rev.* B **44** 545
[9] Takemura K and Fujihisa H 1993 *Phys. Rev.* B **47** 8465
[10] Schulte O and Holzapfel W B 1997 *Phys. Rev.* B **55** 8122
[11] Takemura K, Kobayashi K and Arai M 1998 *Phys. Rev.* B **58** 2482
[12] Degtyareva O, McMahon M I, Allan D R and Nelmes R J 2004 *Phys. Rev. Lett.* **93** 205502
[13] Meenakshi S, Godwal B K, Rao R S and Vijayakumar V 1994 *Phys. Rev.* B **50** 6569
[14] Simak S I, Haeussermann U, Ahuja R, Lidin S and Johansson B 2000 *Phys. Rev. Lett.* **85** 142
[15] Mikhaylushkin A S, Häussermann U, Johansson B and Simak S I 2004 *Phys. Rev. Lett.* **92** 195501
[16] Sin'ko G V and Smirnov N A 2006 *Phys. Rev.* B **74** 134113
[17] Mikhaylushkin A S, Simak S I, Johansson B and Häussermann U 2002 *Phys. Rev.* B **72** 134202
[18] Dmitriev V P, Chernyshov D, Filinchuk Y E and Degtyareva V F 2007 *Phys. Rev.* B **75** 024111
[19] Heine V and Weaire D 1970 Pseudopotential theory of cohesion and structure *Solid State Physics* vol 24 (New York: Academic) p 409 , 459
[20] Degtyareva V F 2006 *Usp. Fiz. Nauk* **176** 383
Degtyareva V F 2006 *Phys.—Usp.* **49** 369 (Engl. Transl.)
[21] Degtyareva V F, Degtyareva O, Winzenick M and Holzapfel V B 1999 *Phys. Rev.* B **59** 6058
[22] Degtyareva V F, Degtyareva O, Holzapfel V B and Takemura K 2000 *Phys. Rev.* B **61** 5823
[23] Degtyareva V F, Degtyareva O, Porsch F and Holzapfel V B 2001 *J. Phys.: Condens. Matter* **13** 7295
[24] Degtyareva V F, Degtyareva O, Porsch F and Holzapfel V B 2002 *J. Phys.: Condens. Matter* **14** 389
[25] Degtyareva V F and Degtyareva O 2002 *J. Phys.: Condens. Matter* **14** 407
[26] Degtyareva V F, Bdikin I K, Porsch F and Novokhatskaya N I 2003 *J. Phys.: Condens. Matter* **15** 1635
[27] Olijnyk H and Holzapfel W B 1984 *J. Physique Coll.* **45** c8 153
[28] Degtyareva V F, Winzenick M and Holzapfel V B 1998 *Phys. Rev.* B **57** 4975
[29] Benedict U 1995 *J. Alloys Compounds* **223** 216